Int. J. Environ. Sci. Technol. (2016) 13:2415–2426
DOI 10.1007/s13762-016-1080-6

ORIGINAL PAPER

Chemical treatment of teff straw by sodium hydroxide, phosphoric acid and zinc chloride: adsorptive removal of chromium

A. B. Wassie[1] · V. C. Srivastava[1]

Received: 12 February 2016 / Revised: 16 June 2016 / Accepted: 23 July 2016 / Published online: 10 August 2016

Abstract In this study, teff (*Eragrostis tef*) straw has been chemically treated and tested as an adsorbent for Cr(VI) removal. Chemically treatment of teff straw was done by NaOH, H_3PO_4 and $ZnCl_2$ solutions. Scanning electron micrograph and X-ray diffraction were used for anatomical characterization, whereas Fourier transform infrared spectroscopy was used for surface change characterization of adsorbents. Effects of different experimental parameters like pH (2–12), initial Cr(VI) concentration (100–900 mg/L), adsorbent dose (2.5–20 g/L), contact time (15–360 min) and temperature (288–318 K) were studied. Temperature increment was found to stimulate the adsorption process. Langmuir isotherm was found to give better representation over wide range of temperature for untreated, H_3PO_4- as well as $ZnCl_2$-treated teff straw, and Freundlich isotherm best represented the isotherm data for NaOH-treated teff straw. Maximum Cr(VI) adsorption capacity of untreated, NaOH-, H_3PO_4- and $ZnCl_2$-treated teff straw was found to be 86.1, 73.8, 89.3 and 88.9 mg/g, respectively. Respective values of average effective diffusion coefficient (D_e) were found to be 2.8×10^{-13}, 2.59×10^{-14}, 1.32×10^{-13} and 1.14×10^{-13} m^2/s, respectively. The negative value of ΔG_o for all the adsorbents indicates Cr(VI) spontaneous adsorption. Isosteric heat of adsorption ($\Delta H_{st,a}$) was found to vary with surface coverage (θ). $\Delta H_{st,a}$ increased for untreated, H_3PO_4- and $ZnCl_2$-treated teff straw, and decreased steadily with θ for NaOH-treated teff straw.

Keywords Adsorption kinetics · Chemically modified adsorbent · Chromium removal · Isosteric heat of adsorption · Isotherm study

Introduction

In the last few decades, interest has grown for the use of lignocellulosic materials for different applications (Jeffries and Jin 2000). Lignocellulosic biomass consists cellulose, hemicellulose and lignin which when separated can be used for different applications. Several types of pretreatment including physical (milling and grinding); chemical (acid, alkaline, oxidizing agent and organic solvent treatment); biological; and combination of physical and chemical techniques (steam pretreatment or auto hydrolysis, hydrothermolysis and wet oxidation) can be used for this purpose. Chemical pretreatment is one of the more efficient and cost-effective methods (Limayem and Ricke 2012; Agbor et al. 2011; Mosier et al. 2005).

Acid hydrolysis, alkaline hydrolysis, use of oxidation agent, organosolv method and ionic liquids can be used for chemical treatment depending upon the end-use. Acid pretreatment solubilizes hemicellulose and cellulose via hydrolysis reaction. Lignin is not hydrolyzed by acid, but it can be made soluble by alkali treatment, while organosolv treatment mainly focuses on solubilization of carbohydrates, and ionic liquid can dissolve both carbohydrates and lignin. Zinc chloride ($ZnCl_2$) is highly effective swelling reagent for biomass, separates hemicellulose from biomass

Editorial responsibility: J. Trögl

Electronic supplementary material The online version of this article (doi:10.1007/s13762-016-1080-6) contains supplementary material, which is available to authorized users.

✉ V. C. Srivastava
vimalcsr@yahoo.co.in

[1] Department of Chemical Engineering, Indian Institute of Technology Roorkee, Roorkee, Uttarakhand 247667, India

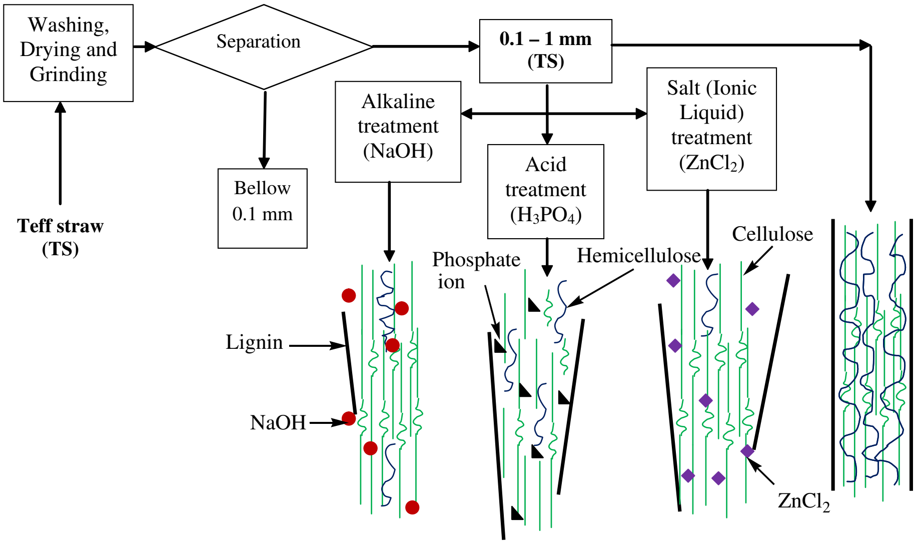

Fig. 1 Flow diagram of chemical treatment on teff straw

(Simkovic et al. 1994), and is highly selective for hemicellulose hydrolysis (Cao et al. 1995a). Zinc–cellulose complexes, formed due to reaction of zinc ions with carbohydrates, could be easily acid hydrolyzed. Acid hydrolysis hydrolyzes hemicellulose to monosaccharides (Cao et al. 1995b).

Chromium-based compounds are used in leather tanning, metal finishing and electroplating industries. Tanning industry is one of major polluting industries in developing countries such as India and Ethiopia (Wassie and Srivastava 2016). Environmental studies have shown that chromium is one of the most toxic dangerous heavy metal (Ali and Aboul-Enein 2002, 2006). Various researchers have reported Cr concentrations in the range of 500–1000 mg/l in untreated effluent from tanneries (Aravindhan et al. 2004; Garg et al. 2012). In Ethiopia, currently there are more than 30 tanneries under operation. From these tanneries, 2–40 mg/L concentration of chromium discharge has been reported (Wassie and Srivastava 2016). This is above the maximum concentration limit set by World Health Organization (WHO). For hexavalent chromium, discharge limit for surface water is 0.1 mg/L and that for potable water is 0.05 mg/L (WHO 2008).

Teff (*Eragrostis tef*) is one of the major food crops used in Ethiopia, and its annual yield is estimated to be about 15.5 million tones/year (Wassie and Srivastava 2016). Teff has very high amount of calcium content and is an excellent source of vitamin C. In the literature, a number of agricultural residues have been tested as adsorbent for chromium removal (Ali and Gupta 2006; Ali 2010, 2012; Ebrahimi et al. 2015; Kunquan et al. 2015; Shiow-Tien et al. 2014; Venkatesan et al. 2014; Doan et al. 2008; Martinez et al. 2015; Huang et al. 2015; Santos et al. 2016; Ali 2012; Elwakeel 2010). However, only few studies have been reported on use of teff straw as an adsorbent because of its less familiarity in scientific research world (Mulu 2013; Bezuayehu et al. 2014). Moreover, in these studies, only minor characterization like Fourier transform infrared (FTIR) of the teff straw was reported and detailed isotherm and thermodynamics were not reported.

Wassie and Srivastava (2016) used raw teff straw without any chemical modification for Cr(VI) removal. Since, chemical modifications are known to improve the characteristics of the adsorbents; therefore, this paper focuses on analyzing effect of chemical treatment on surface functional groups and anatomical structure of teff straw. Chemically treatment of teff straw was done by NaOH, H_3PO_4 and $ZnCl_2$ solutions. Batch experiments have been performed to study the effects of pH (2–12), initial Cr(VI) concentration (100–900 mg/L), adsorbent dose (2.5–20 g/L), contact time (15–360 min) and temperature (288–318 K). Detailed kinetics, isotherm and thermodynamic modeling have been done using various models.

Materials and methods

Adsorbent preparation and characterization

Brown teff (mixture of red and white teff) straw collected from Ethiopia was washed with distilled water so as to remove dust. There is some variation on nutritional content between red and white teff seed (Seyfu 1997). The straw is identified as brown teff straw among other red and white teff straw from the residue teff seed during washing. Size of the dried teff straw was reduced in the range of 0.1–0.6 mm (named as untreated teff straw). This untreated teff straw was soaked with chemicals such as NaOH, H_3PO_4 and $ZnCl_2$.

Treatment with chemicals was done by mixing 100 g/L teff straw in chemical solutions for 2 h at 150 rpm for each chemical. Dried samples were subjected to washing with warm 0.5 N HCl solutions and followed by warm distilled water washing until pH became neutral. Straw to chemical weight ratio of 1:1 was used separately during modification and acid wash. Then the modified samples were named as NaOH, H_3PO_4 and $ZnCl_2$ treated teff straw. Figure 1 shows the flow chart of the modification process.

Elemental analysis was done using VarioMICRO CHNS analyzer. QUANTA Model 200 FEG USA scanning electron microscopy (SEM) was used for morphology analysis. Phillips diffraction unit (Model PW 1140/90) was used for X-ray diffraction (XRD) study of adsorbent. PerkinElmer (Pyris Diamond) thermo-gravimetric (TG) analyzer in temperature range from 20 to 1000 °C at a heating rate of 5 °C/min under both an air and inert atmosphere was used for thermal decomposition analysis. Pellet (pressed-disk) technique was used over a spectral wave number range of 4000 to 400 cm^{-1} for FTIR analysis using Thermo Nicolet, model Magna 760.

Adsorbate preparation and analytical measurement

Potassium dichromate ($K_2Cr_2O_7$) was dissolved in distilled water to prepare aqueous solution of Cr(VI). Analytical reagent-grade potassium dichromate ($K_2Cr_2O_7$) was obtained from Ranbaxy Chemicals Ltd. India. UV−visible spectrophotometer (HACH DR 5000, USA) was used to determine chromium concentrations before and after treatment according to a standard colorimetric method in which absorbance of a pink complex formed between 1, 5-diphenylcarbazide and Cr(VI) was measured at 540 nm wavelength.

Batch experimental procedure

In every experiment, fixed amount of teff straw was added to 50 mL solution with known initial concentration and pH. After the experiment, residual amount of chromium in the supernatant was determined. Adsorption experiments with the teff straw were carried out in batch phases with optimization of one parameter at a time. First effect of pH was studied, in which pH of the 100 mg/L initial Cr concentration solution was varied in the range of 2–12 using 0.1 M HCl and 0.1 M NaOH. Experiments were carried out with buffer solution (citric acid, sodium hydroxide and chloride acid) which provided high buffer capacity with maximum deviation of <5 % from the adjusted pH value. Adsorbent dose was kept constant at 10 g/L, and contact time was 4 h. Similarly, effect of adsorbent dose was studied in the range of 2.5–20 g/L with 100 mg/L initial Cr(VI). For kinetic study, contact time was varied in the range of 15–360 min. Adsorption isotherm experiments were carried out by varying the initial Cr concentrations (100–900 mg/L) with constant adsorbent dose of 10 g/L for 6 h at various temperatures of 15, 25, 35 and 45 °C. Shaking speed of 150 rpm in orbital shaking incubator was used for all experiments. Each experiment was done at least twice, and the average value has been used for calculation. For experimental error $\geq \pm 5$ %, the experiment was redone.

Removal efficiency and the adsorption uptake in solid phase (q_t, mg/g) were calculated using the following relationships:

$$\text{Removal efficiency}\,(\%) = \frac{(C_o - C_t)}{C_o}100 \tag{1}$$

$$q_t = \frac{(C_o - C_t)}{m}V \tag{2}$$

where, C_o and C_t represent the initial and final Cr(VI) concentration (mg/L), t represents contact time, V represents volume of adsorbate solution (L) and m represents the mass of teff straw (g).

Results and discussion

Adsorbent characterization

Scanning electron microscopy (SEM) images of untreated and chemically treated teff straw are shown in Figure S1 at 500 times magnification. Comparison of raw teff straw image with that of NaOH-modified teff straw image shows clear difference in the surface morphology. NaOH-modified teff straw shows structure failure and cellulose dominant biomass. Phosphoric acid- and zinc chloride-modified teff straw show better porosity without much solid structure failure. SEM images (Figure S1) support removal of hemicelluloses after phosphoric acid treatment, removal of lignin and hemicelluloses with cellulose swelling from sodium hydroxide treatment, and selective removal of hemicelluloses from zinc chloride treatments (Cao et al. 1995a; Lopez-Linares et al. 2013; Taherdanak and Zilouei 2014; Xu et al. 2010).

Different studies show separate decomposition assumption for biomass components. First pectin decomposition occurs between 200 and 230 °C, followed by hemicellulose up to 270 °C then celluloses (240–350 °C) and finally lignin (280–500 °C) (Mall et al. 2006). Thermal decomposition for untreated and chemically treated teff straw obtained by pyrolysis is shown in Figure S2. Alkaline, NaOH-treated straw TG graph shows sharp loss of mass of about 5 % (ash percentage) around 310 °C because of non-availability of lignin component, while other acids

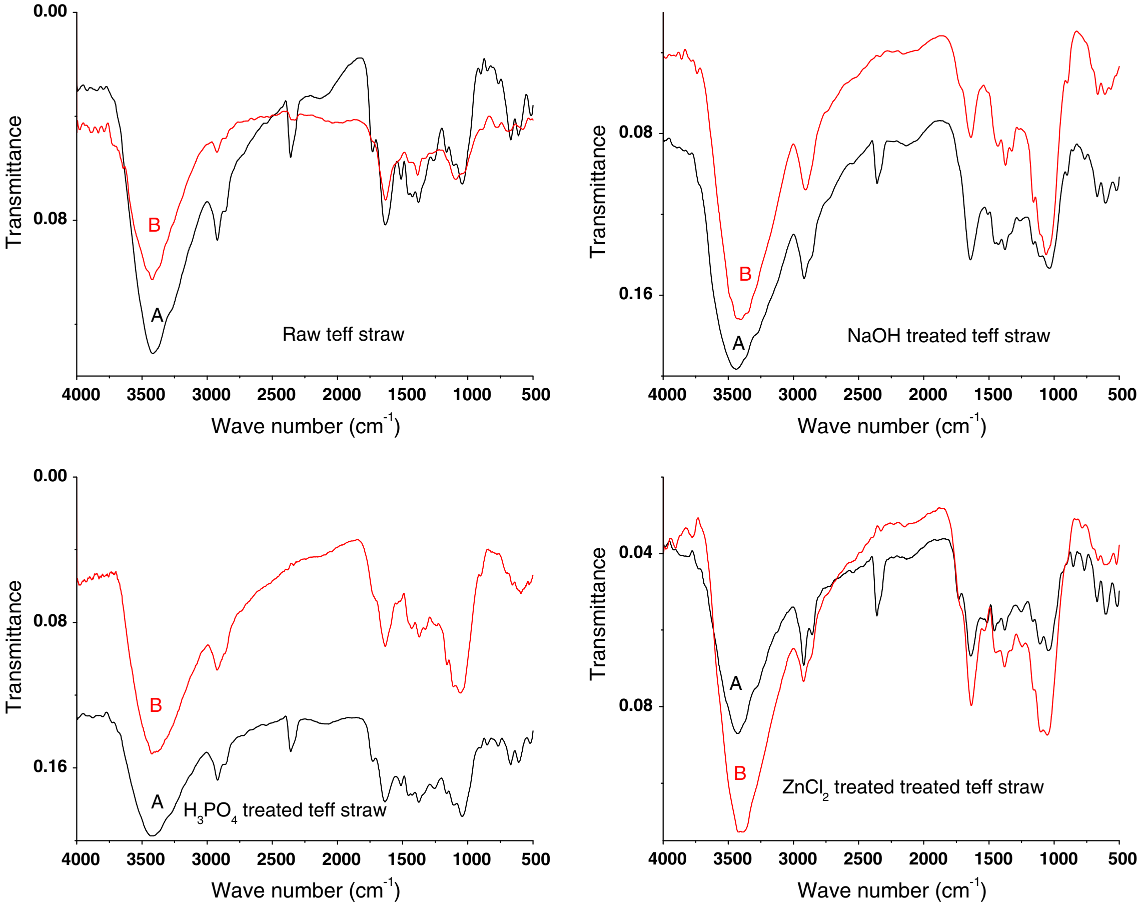

Fig. 2 FTIR spectra of adsorbents (*A*) before and (*B*) after chromium loading

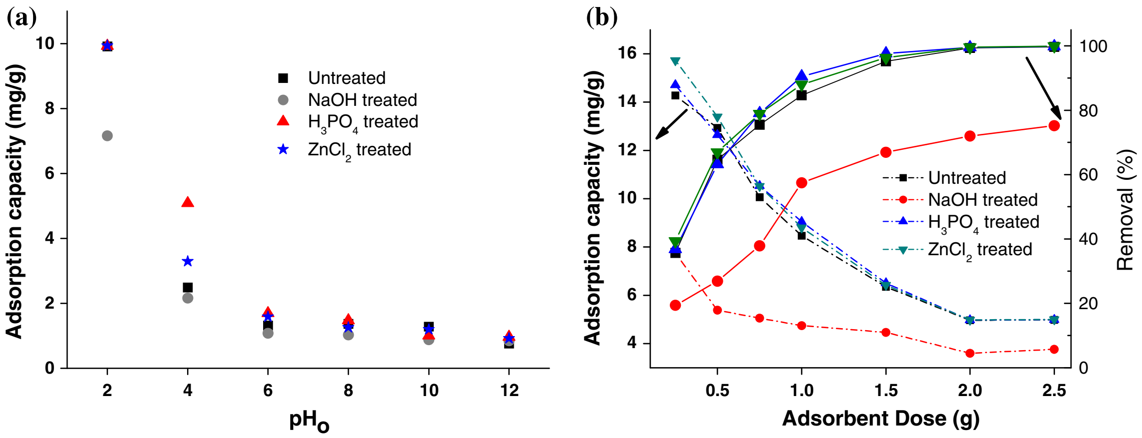

Fig. 3 Effect of **a** pH, and **b** adsorbent mass on the adsorption of Cr(VI) by untreated and chemically treated teff straw ($T = 25$ °C, $t = 4$ h, $m = 10$ g/L, $C_o = 100$ mg/L)

and $ZnCl_2$ treated show 30–40 % loss of mass of lignin and cellulosic component. Table S1 shows summary of thermogravimetric analysis for teff straw and its chemically treated derivatives.

Figure S3 shows the XRD diffraction patterns of raw and chemically treated samples of teff straw. Main peak appearing at 2θ value of ~22° indicates of the distance between hydrogen-bonded sheets in cellulose. Broad peak observed ~16° is known to be a composite of two peaks from I_β (16.7° and 14.9°), I_α (16.8° and 14.3°) or both (Yang et al. 2007). Small peak at 34.5° may be due to ordering of one cellobiose unit along the fiber direction.

Crystallinity index (CrI) is the measurement of fraction of crystalline material. CrI can be estimated using intensity of the peak at ~22° (as main peak) and the intensity of the peak at ~18° (between the main peak and the secondary peak at ~16°) due to the amorphous portion:

$$\mathrm{CrI} = \frac{I_{\mathrm{Total}} - I_{\mathrm{Amorphous}}}{I_{\mathrm{Total}}} \tag{3}$$

Relative change in CrI for unmodified and modified teff straw adsorbents is shown in Table S1. The CrI of untreated teff straw was found to be 52.01 %. There is an increase in CrI to 61.31 % for NaOH-treated teff straw due to the relatively high percentage amorphous removal (such as lignin) than other types of chemical treatment (Ngah et al. 2008). Debye–Scherrer equation (Eq. 4) was used to estimate crystallite size (Langford and Wilson 1978):

$$B(2\theta) = \frac{K\lambda}{L\cos\theta} \tag{4}$$

where, B is the breadth of the peak at half height (rad) of a specific phase (in this case at $2\theta = 22.2$, 22.3, 22 and 21.8 for raw, NaOH treated, H_3PO_4 treated, and $ZnCl_2$ treated, respectively), $K = 0.94$), λ (1.542 Å) is the wavelength of X-ray, θ is the center angle of the peak and L is the crystallite length. For raw, NaOH-treated, H_3PO_4-treated and $ZnCl_2$-treated teff straw, FWHM was 26×10^{-3}, 9×10^{-3}, 10×10^{-3} and 33×10^{-3} rad, respectively, and corresponding crystalline size was found to be about 110, 320, 290 and 90 Å. XRD analysis shows that alkaline and acid treatment results in decrease in peak width and increase in its magnitude. This is due to amorphous lignin removal and higher crystallinity level of hydrolyzed cellulose (Park et al. 2010).

FTIR analysis is an important technique for identifying functional groups which help in adsorbing metal ions. Each part of biomass has different types and amount of functional groups which may be used in heavy metal adsorption. For example, aromatic rings and hydroxyl functional groups are dominantly available in lignin component of the biomass. Figure S4 highlights the percentage importance of each binding group in the mechanism of metal ion adsorption in the literature (Nurchi and Villaescusa 2011). Therefore, it is expected that peak strength increases in some functional groups due to the increment in surface area and loss of certain functional group due to removal of certain lignocellulosic part during chemical modification. Figure S5 shows the FTIR graph of raw and chemically treated teff straw. Compared to raw teff straw, the peak around 1730 cm^{-1} (due to carboxylic and carbonyl groups from aldehydes, ketones as well as aromatic rings mainly from lignin part) is not observed in NaOH-treated teff straw and shows intensity reduction for other chemical treatments due to lignin removal during the treatments. Amine group and C–H functional group from $ZnCl_2$-treated teff straw show intensity reduction due to zinc and chloride ions reaction to these functional groups. Figure 2 shows the effect of chromium loading on the functional groups. Almost all functional groups show reduction in peak intensity with respect to chromium-loaded raw teff straw, while few peaks show intensity reduction during chromium loading on chemically treated teff straw. Extra capacity to handle more chromium loading in chemically treated teff straw than that in raw teff straw is due to the surface area improvement and surface functional groups increment. Observed peaks and their assigned functional groups due to chemical treatment and chromium loading have been summarized in Table S2 (Cheng et al. 2011; Teixeira et al. 2004; Mishra and Jha 2009).

Adsorption parameter effects

Solution pH can affect the adsorption process by affecting the speciation of metal in the solution and by changing the state of the active binding sites on biomass like teff straw. When the pH was decreased from 6 to 2, Cr(VI) sorption increased rapidly (Fig. 3a). It can be seen that no signification adsorption of Cr(VI) at pH greater than 6.0 was observed. This is because of the competition of OH^- of aqueous solution with the anions species of hexavalent chromium for the adsorption sites.

Table 1 Pseudo-first- and pseudo-second-order parameters for the adsorption of Cr(VI) on different chemical treated adsorbent prepared from teff straw

Adsorbent from teff straw	Kinetics parameters						
	Pseudo-first-order $\frac{dq_t}{d_t} = k_1(q_e - q_t)$			Pseudo-second-order $\frac{dq_t}{d_t} = k_2(q_e - q_t)^2$			
	K_1 (1/min)	q_e (mg/g)	R^2	K_2 (g/mg min) × 10^3	q_e (mg/g)	h (mg/g min)	R^2
Untreated	0.060	59.29	0.703	1.47	11.23	0.188	0.995
NaOH treated	0.051	64.73	0.586	0.18	13.99	0.034	0.745
H_3PO_4 treated	0.069	97.27	0.786	1.03	11.85	0.144	0.990
$ZnCl_2$ treated	0.081	122.72	0.875	1.56	11.11	0.193	0.997

q_e is the concentration Cr(VI) adsorbed at equilibrium; q_t is the concentration Cr(VI) adsorbed at time t; k_1 is rate constant for pseudo-first-order equation; and k_2 is the second-order rate constant for the pseudo-second-order equation

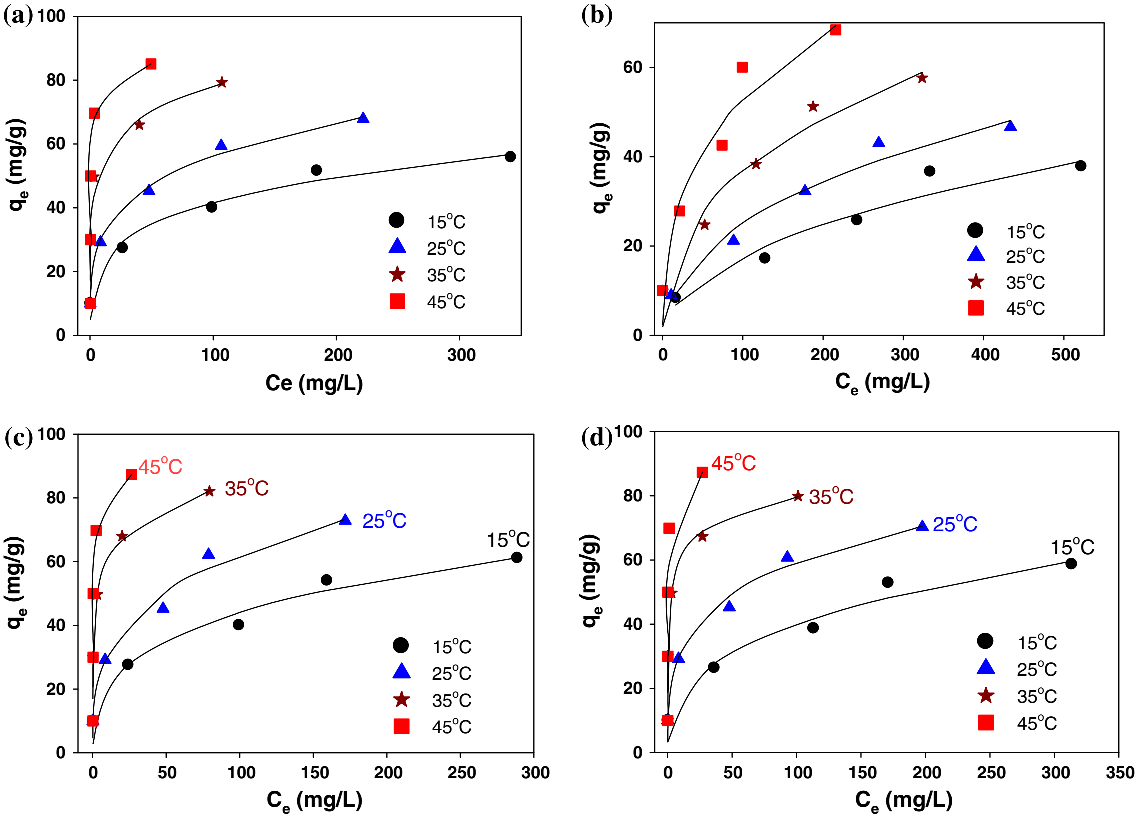

Fig. 4 Equilibrium adsorption isotherms at different temperatures for teff straw system, **a** untreated, **b** NaOH-treated, **c** H_3PO_4-treated and **d** $ZnCl_2$-treated teff straw. Experimental data points given by the *symbols* and the *lines* predicted by the best-fit isotherm model; pH_o: 2.0; *m*: 10 g/L

Effect of teff straw dosage on removal of Cr(VI) is shown in Fig. 3b. When the amount of teff straw added increased the sorption rate of Cr(VI) also increased. Except NaOH-treated teff straw, chromium removal efficiency was above 85 % at 10 g/L. At higher dose of teff straw, removal efficiency became stable showing a low sorption rate increment per increment of straw adsorbent dose. Also at higher dose, more sorption sites are available without saturation; however, due to the fixed total chromium quantity which is available for removal, Cr adsorption per mass of straw adsorbent decreased at higher dosage.

The contact time for exchange of adsorbate from solution to the adsorbent is very important factor in the adsorption treatment process. Uptake of Cr(VI) species was initially fast due to the large availability of vacant surface sites, and uptake rate became slow when the adsorption reached equilibrium. There was fast removal over 50 % in the first hour and reached above 90 % in 4 h for H_3PO_4, $ZnCl_2$ and untreated (raw) teff straw adsorbent. Removal efficiency was found to be comparatively less (about 20 % in 1 h and 70 % in 6 h) for NaOH-treated teff straw.

NaOH-treated teff straw showed low removal efficiency mainly because removal of amorphous lignin during the treatment with NaOH caused structural failure and loss of significant amount of functional groups that have high affinity toward metal ions.

Adsorption kinetics

Adsorption rate is described by adsorption kinetics which is an important characteristic for evaluating the adsorption process. In this study, pseudo-first-order and pseudo-second-order models were applied (Gurgel et al. 2009). When sorption rate follows an assumption that the rate of occupation of adsorption sites is proportional to the square of number of unoccupied sites, it is called pseudo-second-order kinetic rate (Ho 2004; Ho and McKay 1998). Both equations are given in Table 1. Kinetic parameter values are shown in Table 1 for both pseudo-first-order and pseudo-second-order kinetics. R^2 values show pseudo-second-order kinetics gave better fitting than pseudo-first-order kinetics model and high initial adsorption rate, ($k_2q_e^2$), value from $ZnCl_2$-treated and untreated teff straw adsorbent 0.193 and 0.188 mg/g min, respectively, and for NaOH-treated teff straw, the initial adsorption rate is only 0.034 mg/g min.

Table 2 Isotherm parameters for Cr(VI) adsorption onto teff straw adsorbents at different temperatures

Temperature (K)	Untreated			NaOH treated			H_3PO_4 treated			$ZnCl_2$ treated		
Langmuir $q_e = \frac{q_{max} b C_e}{1+bC_e}$	q_{max} (mg/g)	b (L/mg)	R^2	q_{max} (mg/g)	b (L/mg)	R^2	q_{max} (mg/g)	b (L/mg)	R^2	q_{max} (mg/g)	b (L/mg)	R^2
288	58.4	0.0426	0.986	47.9	0.0066	0.897	64.3	0.0360	0.965	62.9	0.0282	0.956
298	70.1	0.0763	0.988	57	0.0095	0.950	76.3	0.0679	0.971	73.1	0.0716	0.982
308	79.3	0.4470	0.995	63.6	0.0209	0.935	83.2	0.5611	0.998	80.6	0.5277	0.998
318	86.1	1.6597	0.999	73.8	0.0385	0.947	89.3	1.7157	0.999	88.9	2.0022	0.999
Freundlich $q_e = k_f C_e^{1/n}$	k_f (L/mg)	n	R^2	k_f (L/mg)	n	R^2	k_f (L/mg)	n	R^2	k_f (L/mg)	n	R^2
288	13.7	4.2	0.992	2.2	2.2	0.964	13.8	4.0	0.984	13.4	4.1	0.966
298	17.2	3.9	0.999	2.9	2.2	0.988	17.3	3.7	0.991	17.2	3.8	0.996
308	28.3	4.0	0.805	13	4.3	0.937	29.3	3.6	0.826	28.7	3.9	0.813
318	37.7	3.6	0.646	16	4	0.958	40.4	3.1	0.669	42.1	3.2	0.613

Determination of diffusivity

Boyd et al. (1947) model (assuming the adsorbent particles to be spherical having radius (R_a, m)), given by following expression, could be used to determine the effective diffusion coefficient (D_e, m^2/s) from the kinetic data:

$$F(t) = 1 - \frac{6}{\pi^2} \sum_{z=1}^{\infty} \frac{1}{z^2} \exp\left(\frac{-z^2 \pi^2 D_e t}{R_a^2} \right) \tag{5}$$

where, $F(t)=q_t/q_e$ is at time t, and z is an integer. The average radius from sieve analysis is 0.15 mm for raw teff straw and its chemically impregnated derivatives as: 0.07 mm for NaOH and about 0.1 mm for both H_3PO_4 and $ZnCl_2$ impregnated. Vermeulen's approximation (Vermeulen 1953) given by Eq. (5) fits the whole range $0 < F(t) < 1$.

$$F(t) = \left[1 - \exp\left(\frac{-\pi^2 D_e t}{R_a^2} \right) \right]^{1/2} \tag{6}$$

This equation could further be simplified for calculating D_e.

$$\ln\left[\frac{1}{(1 - F^2(t))} \right] = \frac{\pi^2 D_e t}{R_a^2} \tag{7}$$

Thus, D_e is obtained from the slope of $\ln[1/(1-F^2(t))]$ versus t plot. The average values of D_e has been found to be 2.8×10^{-13}, 2.59×10^{-14}, 1.32×10^{-13} and 1.14×10^{-13} m^2/s for raw, NaOH-, H_3PO_4- and $ZnCl_2$-treated teff straw adsorbents, respectively.

Effect of temperature

Figure 4 shows plots of adsorption isotherms for Cr(VI)–teff straw adsorbents at different temperatures of 288, 298, 308 and 318 K. It is observed that the sorption of Cr(VI) increased with an increase in temperature. This is because an increase in temperature increases the mobility of Cr(VI) with better diffusion characteristics. This results in enhancement in the adsorptive capacity of the adsorbent. However, during the adsorption process, diffusion of the metal ions through the pores of the adsorbents is not the only rate-controlling step; therefore, the endothermic nature of the adsorption may be due to chemisorptive nature of the adsorption process.

Adsorbent binding site characteristics like structure, functional groups, surface properties; and nature of adsorbates such as molecular structure, concentration, standard redox potential, size, weight, as well as charge of the ion are important factors in addition to solution chemistry (like ionic strength, pH).

Adsorption equilibrium study

The experimental adsorption equilibrium isotherm data have been fitted to Langmuir and Freundlich models. Langmuir isotherm is based on assumption that sorption will take place at specific homogeneous sites of the adsorbents, while Freundlich isotherm considers heterogeneous and non-uniform heat of adsorption distribution on the adsorbent surface (Srivastava et al. 2007). Both equations and their respective parameters, and R^2 values are shown in Table 2. Langmuir isotherm represents most of the adsorption data at wide variety of temperature range for untreated and H_3PO_4- and $ZnCl_2$-treated teff straw adsorbent, while Freundlich isotherm shows slightly better fitting for NaOH-treated teff straw adsorbent and at 288 K.

Estimation of thermodynamic parameters

Classical thermodynamics gives the following relationship between Gibbs free energy change (ΔG_o, kJ/mol), the

Table 3 Thermodynamic parameters for Cr(VI) adsorption onto teff straw adsorbents

Temperature (K)	Untreated				NaOH treated				H_3PO_4 treated				$ZnCl_2$ treated			
	K_D (L/g)	ΔG_0 (kJ/mol)	ΔH_0 (kJ/mol)	ΔS_0 (J/mol K)	K_D (L/g)	ΔG_0 (kJ/mol)	ΔH_0 (kJ/mol)	ΔS_0 (J/mol K)	K_D (L/g)	ΔG_0 (kJ/mol)	ΔH_0 (kJ/mol)	ΔS_0 (J/mol K)	K_D (L/g)	ΔG_0 (kJ/mol)	ΔH_0 (kJ/mol)	ΔS_0 (J/mol K)
288	42.3	−8.966	34.25	150.07	0.06	6.66	195.63	656.14	39	−8.784	36.02	155.56	40	−8.833	35.58	154.22
298	68.3	−10.467			0.96	0.098			64.9	−10.339			65.9	−10.374		
308	107.1	−11.967			12.5	−6.463			104.1	−11.895			105	−11.917		
318	163	−13.468			137.9	−13.025			162	−13.450			162.5	−13.459		

entropy change (ΔS_o, kJ/mol K) and the enthalpy change (ΔH_o, kJ/mol):

$$-\frac{\Delta G_o}{RT} = \frac{\Delta S_o}{R} - \frac{\Delta H_o}{RT} = \ln K_D \tag{8}$$

where, K_D (q_e/C_e) is linear sorption distribution coefficient obtained from the intercept of the ln(q_e/C_e) versus q_e plot. ΔH_o (also called isosteric heat of adsorption ($\Delta H_{st,o}$) with zero surface coverage) was determined from the slope of ln K_D versus (1/T) plot (Suzuki and Fujii 1982). Values of ΔG_o, ΔH_o and ΔS_o have been estimated and are shown in Table 3. ΔH_o was found to be positive indicating endothermic adsorption process. This may be due to the fact that metal ions have to displace water and other molecules for its adsorption. The positive value and magnitude of ΔS_o tell the degree of randomness at the adsorbent–solution interface and an affinity of the adsorbents toward Cr(VI) ions. ΔG_o values were negative indicating the spontaneous and feasible adsorption process.

Isosteric heat of adsorption

For constant q_e (10, 20, 30, 40, 50 mg/g) of teff straw adsorbents, the apparent isosteric heat of adsorption ($\Delta H_{st,a}$) was calculated using Clausius–Clapeyron equation (Raymon 1998):

$$\frac{-\Delta H_{st,a}}{RT^2} = \left[\frac{d \ln C_e}{dT}\right] \tag{9}$$

In this case, C_e at constant q_e at different temperatures was obtained from the best-fit isotherm model which was further used to plot isosters (shown in Fig. 5) at different q_e for Cr(VI). $\Delta H_{st,a}$ values (calculated from slope of the lnC_e versus (1/T) plot) and R^2 values are presented in Table 4. R^2 values shown in Table 4 confirm good representation of experimental data by Eq. (9). Figure S6 shows that values of $\Delta H_{st,a}$ varies with surface loadings for Cr(VI)–adsorbent systems indicating heterogeneous nature of the adsorbent surface. It may be noted that the $\Delta H_{st,a}$ is obtained after subtracting the heat of solution (ΔH_{sol}) and the heat of adsorption of water (ΔH_w) from the net isosteric heat of adsorption ($\Delta H_{st,net}$):

$$\Delta H_{st,a} = \Delta H_{st,net} - \Delta H_{sol} - f\Delta H_W \tag{10}$$

where, f is the number of moles of water exchanged per mole of adsorbate. ΔH_w is normally assumed to be zero, and ΔH_{sol} for potassium dichromate is 17.4 kJ/mol. $\Delta H_{st,net}$ values calculated from Eq. (10) are given in Table 4.

Regeneration study

Regeneration of spent untreated and chemically treated teff straw was carried out by washing them three times

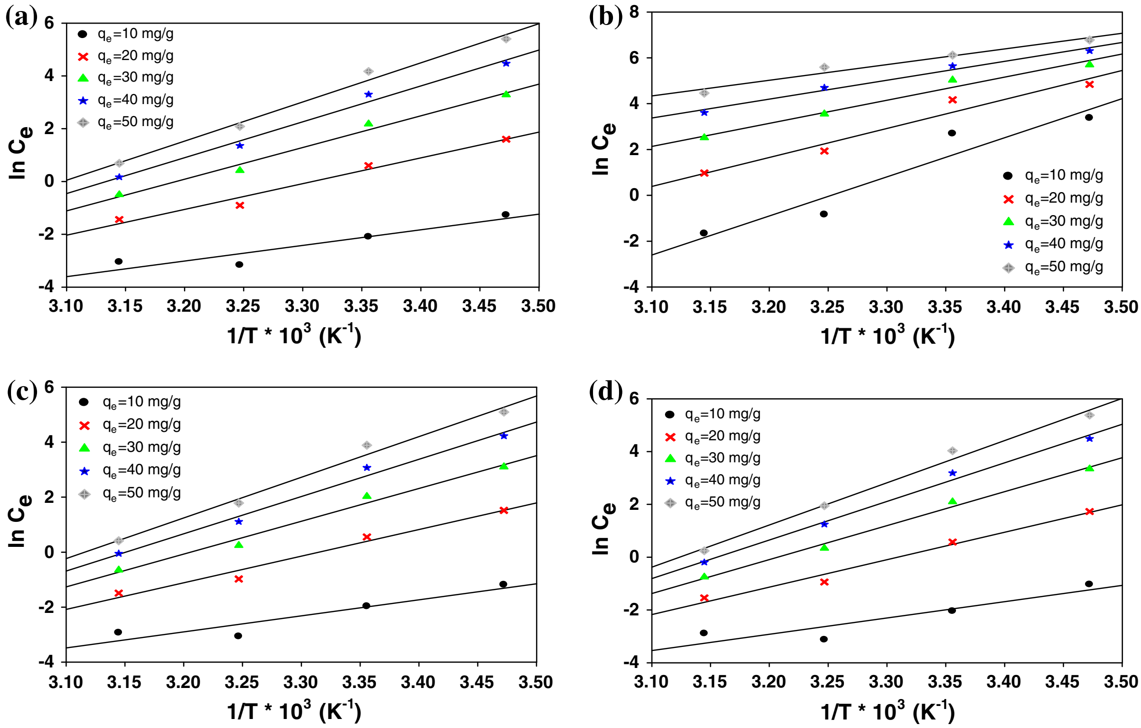

Fig. 5 Adsorption isosters' for determining isosteric heat of adsorption, **a** untreated, **b** NaOH-treated, **c** H_3PO_4-treated, **d** $ZnCl_2$-treated teff straw

Table 4 Isosteric enthalpy for Cr(VI) adsorption onto teff straw adsorbents

q_e (mg/g)	Untreated			NaOH treated			H_3PO_4 treated			$ZnCl_2$ treated		
	$\Delta H_{st,a}$ (kJ/mol)	$\Delta H_{st,net}$ (kJ/mol)	R^2	$\Delta H_{st,a}$ (kJ/mol)	$\Delta H_{st,net}$ (kJ/mol)	R^2	$\Delta H_{st,a}$ (kJ/mol)	$\Delta H_{st,net}$ (kJ/mol)	R^2	$\Delta H_{st,a}$ (kJ/mol)	$\Delta H_{st,net}$ (kJ/mol)	R^2
10	5.92	23.32	0.880	17.06	34.46	0.916	5.84	23.24	0.874	6.16	23.56	0.839
20	9.75	27.15	0.976	12.65	30.05	0.954	9.69	27.09	0.973	10.39	27.79	0.981
30	11.99	29.39	0.986	10.08	27.48	0.976	11.93	29.33	0.985	12.86	30.26	0.992
40	13.59	30.99	0.988	8.25	25.65	0.981	13.53	30.93	0.987	14.62	32.02	0.992
50	14.82	32.22	0.988	6.83	24.23	0.962	14.77	32.17	0.987	15.98	33.38	0.990

with hot water (383 K) and followed by washing with 0.1 M H_2SO_4 solution (20 g spent adsorbent in one liter for 30 min). This adsorption–regeneration cycle was performed for four number of cycles (Fig. 6). The considerable improvement in Cr(VI) removal efficiencies was observed for NaOH-treated adsorbent after hot water–H_2SO_4 solution regeneration (Fig. 6a). This may be due to change in adsorbent surface pH chemistry. Approximately, 60–80 % mass recovery (with respect to the initial adsorbent mass) was observed after the fourth cycle (Fig. 6b). This is because of teff straw is tiny in structure, and its residues have a tendency of easily crack into more additional acid solution and hydrothermal solubility of some low polymerized lignin and hemicelluloses as well as other extractives.

Adsorption mechanism and comparative assessment

Cr(VI) removal from aqueous solution by a biomass could be through two mechanisms (Park et al. 2005). In first mechanism, Cr(VI) gets directly reduced to Cr(III) by electron-donor functional groups. In second mechanism, Cr(VI) binds to the positively charged groups like amino and carboxyl groups (their existence in teff straw is confirmed by FTIR analysis) and further gets reduced to Cr(III) (by adjacent electron-donor groups) which further gets released into the aqueous phase due to electronic repulsion between the positively charged groups. Figure 7 shows proposed chromium removal mechanism by teff straw.

A number of studies have been conducted using raw (virgin) plant wastes or biochar as adsorbents. Only few

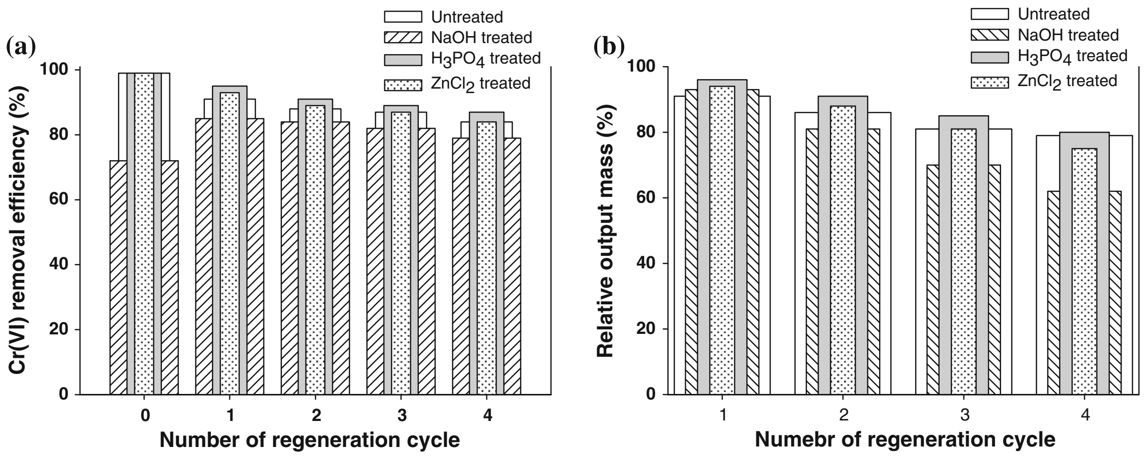

Fig. 6 **a** Cr(VI) removal efficiency, and **b** regenerated adsorbent mass recovery (%) during various cycles of regeneration of the adsorbents by hot water and sulfuric acid solution

Fig. 7 Proposed chromium removal mechanism by teff straw

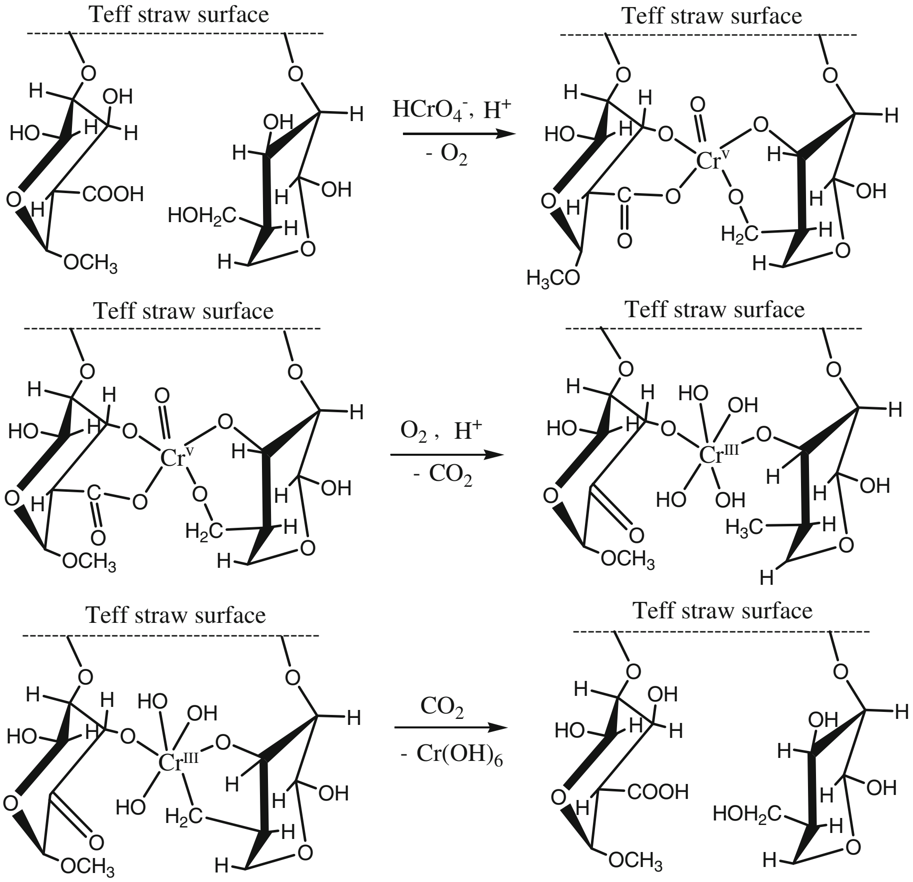

studies are available in which chemical treated plant materials have been used. Comparative assessment of agricultural residues for Cr(VI) removal is shown in Fig. 8 (Sharma and Forster 1994; Dakiky et al. 2002; Gonzalez et al. 2008; Anandkumar and Mandal 2009; Bansal et al. 2009; Dhir and Kumar 2010; Rao and Rehman 2010; Blanes et al. 2016). It may be seen in the figure that adsorption capacity of these biomass-based low-cost adsorbents varies in the range of 5-80 mg/g for adsorption experiments carried out at 298–303 K. Teff straw has better adsorption capacity than most of the adsorbents; however, a few have better adsorption capacity than teff straw as well. It may be noted that a direct comparison of adsorption capacity of these adsorbents is not justified as the adsorption experiments have been carried out different conditions of time, pH, etc. It should be noted that regeneration of the biomass-based adsorbent has not been

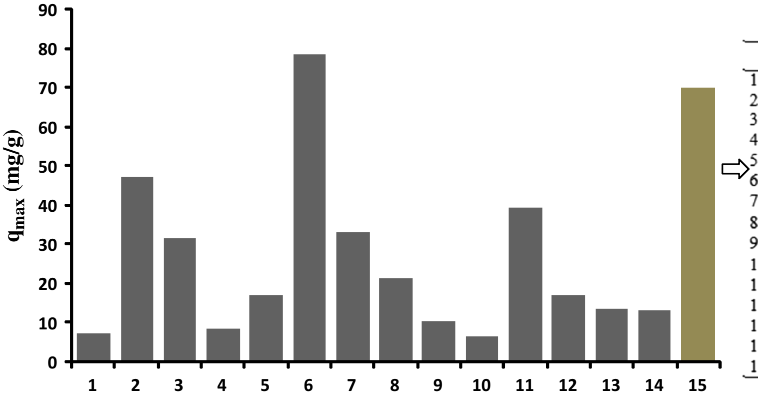

	Material	Source
1	Soy hull	Blanes et al., 2016
2	Wheat straw	Dhir and Kumar, 2010
3	fruits of Gular	Rao and Rehman, 2010
4	Rice husk	Bansal et al., 2009
5	Bael fruit shell	Anandkumar & Mandal., 2009
6	Coconut coir	Gonzalez et al., 2008
7	olive cake	Dakiky et al., 2002
8	pine needles	Dakiky et al., 2002
9	almond shells	Dakiky et al., 2002
10	cactus leaves	Dakiky et al., 2002
11	Sawdust	Sharma and Forster, 1994
12	Sugar beet pulp	Sharma and Forster, 1994
13	Maize cob	Sharma and Forster, 1994
14	Sugarcane bagasse	Sharma and Forster, 1994
15	Teff straw	This work

Fig. 8 Maximum adsorption capacities for virgin biomass residues at 298–303 K

reported in most of the previous studies, and based on the present work, it seems that the teff straw can be reused for four number of cycles with significant adsorption capacity.

Conclusion

Various characterization techniques confirmed removal of hemicelluloses from teff straw after phosphoric acid treatment, removal of lignin and hemicelluloses with cellulose swelling from sodium hydroxide treatment, and selective removal of hemicelluloses from zinc chloride treatment of teff straw. Equilibrium isotherms were analyzed at various temperature ranges, and Langmuir isotherm was found to give good representation over wide range of temperature for untreated, H_3PO_4 treated as well as $ZnCl_2$ treated. For untreated, H_3PO_4-treated, $ZnCl_2$-treated and NaOH-treated teff straw, maximum adsorption capacity from Langmuir isotherm model increased from 58.4, 47.9, 64.3, 62.9 mg/g at 288 K to 86.1, 73.8, 89.3, 88.9 mg/g, respectively, at 318 K. Cr(VI) adsorption onto all the adsorbents was endothermic in nature. The negative value of ΔG_o indicates spontaneous adsorption of Clausius–Clapeyron equation was used for calculation of $\Delta H_{st,a}$ which were low at low surface coverage and increased progressively for untreated, H_3PO_4- and $ZnCl_2$-treated teff straw. For NaOH-treated teff straw, $\Delta H_{st,a}$ was higher at low surface coverage which decreased with increase in adsorption. All the adsorbents showed heterogeneous surface characteristics.

Acknowledgments First author is thankful to the Ministry of Education, Government of Ethiopia, for providing financial sponsorship to do Ph.D. in India.

References

Agbor VB, Cicek N, Sparling R, Berlin A, Levin DB (2011) Biomass pretreatment: fundamentals toward application. Biotechnol Adv 29:675–685

Ali I (2010) The quest for active carbon adsorbent substitutes: inexpensive adsorbents for toxic metal ions removal from wastewater. Sep Purfi Rev 39:95–171

Ali I (2012) New generation adsorbents for water treatment. Chem Rev 112:5073–5091

Ali I, Aboul-Enein HY (2002) Speciation of arsenic and chromium metal ions by reversed phase high performance liquid chromatography. Chemosphere 48(3):275–278

Ali I, Aboul-Enein HY (2006) Instrumental methods in metal ions speciation: chromatography, capillary electrophoresis and electrochemistry. Taylor & Francis Ltd, New York. ISBN 0-8493-3736-4

Ali I, Gupta VK (2006) Advances in water treatment by adsorption technology. Nat Lond 1:2661–2667

Anandkumar J, Mandal B (2009) Removal of Cr(VI) from aqueous solution using Bael fruit (*Aegle marmelos correa*) shell as an adsorbent. J Hazard Mater 168:633–640

Aravindhan R, Madhan B, Rao JR, Nair BU, Ramasami T (2004) Bioaccumulation of chromium from tannery wastewater: an approach for chrome recovery and reuse. Environ Sci Technol 38:300–306

Bansal M, Garg U, Singh D, Garg VK (2009) Removal of Cr(VI) from aqueous solutions using pre-consumer processing agricultural waste: a case study of rice husk. J Hazard Mater 162:312–320

Bezuayehu T, Endale T, Negussie M (2014) The Teff straw: a novel low-cost adsorbent for quantitative removal of Cr(VI) from contaminated aqueous samples. Desalin Water Treat 56:2925–2936

Blanes PS, Bordoni ME, González JC, García SI, Atria AM, Sala LF, Bellú SE (2016) Application of soy hull biomass in removal of Cr(VI) from contaminated waters. Kinetic, thermodynamic and continuous sorption studies. J Environ Chem Eng 4:516–526

Boyd GE, Adamson AW, Meyers LS (1947) The exchange adsorption of ions from aqueous solution by organic zeolites: II kinetics. J Am Chem Soc 69:2836–2848

Cao NJ, Xu Q, Chen LF (1995a) Xylan hydrolysis in zinc chloride solution. Appl Biochem Biotechnol 51(52):97–104

Cao NJ, Xu Q, Chen LF (1995b) Acid hydrolysis of cellulose in zinc chloride solution. Appl Biochem Biotechnol 51(52):21–28

Cheng G, Varanasi P, Li C, Liu H, Melnichenko YB, Simmons BA, Kent MS, Singh S (2011) Transition of cellulose crystalline structure and surface morphology of biomass as a function of ionic liquid pretreatment and its relation to enzymatic hydrolysis. Biomacromolecules 12:933–941

Dakiky M, Khamis M, Manassra A, Mereb M (2002) Selective adsorption of chromium(VI) in industrial wastewater using low-cost abundantly available adsorbents. Adv Environ Res 6:533–540

Dhir B, Kumar R (2010) Adsorption of heavy metals by Salvinia biomass and agricultural residues. Int J Environ Res 4:427–432

Doan HD, Lohi A, Dang VBH, Dang-Vuc T (2008) Removal of Zn^{+2} and Ni^{+2} by adsorption in a fixed bed of wheat straw. Process Safety Environ Prot 86:259–267

Ebrahimi A, Ehteshami M, Dahrazma B (2015) Isotherm and kinetic studies for the biosorption of cadmium from aqueous solution by *Alhaji maurorum* seed. Process Saf Environ Prot 98:374–382

Elwakeel KZ (2010) Removal of Cr(VI) from alkaline aqueous solutions using chemically modified magnetic chitosan resins. Desalination 250:105–112

Garg SK, Tripathi M, Srinath T (2012) Strategies for chromium bioremediation of tannery effluent. In: Reviews of environmental contamination and toxicology, vol 217. Springer, US, pp 75–140

Gonzalez MH, Araújo GC, Pelizaro CB, Menezes EA, Lemos SG, de Sousa GB, Nogueira AR (2008) Coconut coir as biosorbent for Cr(VI) removal from laboratory wastewater. J Hazard Mater 159(2–3):252–256

Gurgel LVA, Melo JCP, Lena JC, Gil LF (2009) Adsorption of chromium(VI) ion from aqueous solution by succinylated mercerized cellulose functionalized with quaternary ammonium groups. Bioresour Technol 100(13):3214–3220

Ho YS (2004) Citation review of Lagergren kinetic rate equation on adsorption reactions. Scientometrics 59:171–177

Ho YS, McKay G (1998) A comparison of chemisorptions kinetic models applied to pollutant removal on various sorbents. Process Safety Environ Protect 76:332–340

Huang K, Xiu Y, Zhu H (2015) Removal of hexavalent chromium from aqueous solution by crosslinked mangosteen peel biosorbent. Int J Environ Sci Technol 12:2485–2492

Jeffries TW, Jin YS (2000) Ethanol and thermotolerance in the bioconversion of xylose by yeast. Adv Appl Microbiol 47:221–268

Kunquan L, Yuan J, Xiaohua W, Di B, Hua L, Zheng Z (2015) Effect of nitric acid modification on the lead(II) adsorption of mesoporous biochars with different mesopore size distributions. Clean Technol Environ Policy. doi:10.1007/s10098-015-1056-0

Langford JI, Wilson AJC (1978) Scherrer after sixty years: a survey and some new results in the determination of crystallite size. J Appl Cryst 11:102–113

Limayem A, Ricke SC (2012) Lignocellulosic biomass for bioethanol production: current perspectives, potential issues and future prospects. Prog Energy Combust Sci 38:449–467

Lopez-Linares JC, Cara C, Moya M, Ruiz E, Castro E, Romero I (2013) Fermentable sugar production from rape seed straw by dilute phosphoric acid pretreatment. Ind Crops Products 50:525–531

Mall ID, Srivastava VC, Agarwal NK (2006) Removal of orange-g and methyl violet dyes by adsorption onto bagasse fly ash-kinetic study and equilibrium isotherm analyses. Dyes Pigments 69:210–223

Martınez LJ, Munoz-Bonilla A, Mazario E, Recio FJ, Palomares FJ, Herrasti P (2015) Adsorption of chromium(VI) onto electrochemically obtained magnetite nanoparticles. Int J Environ Sci Technol 12:4017–4024

Mishra A, Jha B (2009) Isolation and characterization of extracellular polymeric substances from micro-algae Dunaliella salina under salt stress. Bioresour Technol 100(13):3382–3386

Mosier N, Wyman C, Dale B (2005) Features of promising technologies for pretreatment of lignocellulosic biomass. Bioresour Technol 96:673–686

Mulu BD (2013) Batch sorption experiments: Langmuir and Freundlich isotherm studies for the adsorption of textile metal ions onto teff straw (*Eragrostis tef*) agricultural waste. J Thermodyn. doi:10.1155/2013/375830

Ngah WS, Wan KM, Hanafiah MA (2008) Removal of heavy metal ions from wastewater by chemically modified plant wastes as adsorbents: a review. Bioresour Technol 99:3935–3948

Nurchi MV, Villaescusa I (2011) The chemistry behind the use of agricultural biomass as sorbent for toxic metal ions: pH influence, binding groups, and complexation equilibria. In: Matovic D (ed) Biomass - Detection, Production and Usage. In Tech, pp 409–424. ISBN: 978-953-307-492-4. http://www.intechopen.com/books/biomass-detection-production-and-usage/the-chemistry-behind-the-use-of-agricultural-biomass-as-sorbent-for-toxic-metal-ions-ph-influence-bi. Accessed 11 Jan 2016

Park D, Yun Y, Park JM (2005) Studies on hexavalent chromium biosorption by chemically treated biomass of *Ecklonia sp*. Chemosphere 60:1356–1364

Park S, Baker JO, Himmel ME, Parilla PA, Johnson DK (2010) Cellulose crystallinity index: measurement techniques and their impact on interpreting cellulase performance. Biotech Biofuel 3:10

Rao RAK, Rehman F (2010) Adsorption studies on fruits of Gular (Ficus glomerata): removal of Cr(VI) from synthetic wastewater. J Hazard Mater 181:405–412

Raymon C (1998) Chemistry: thermodynamic, vol 737. McGraw-Hill, Boston

Santos FA, Alban L, Frankenberg CLC, Pires M (2016) Characterization and use of biosorbents prepared from forestry waste and their washed extracts to reduce/remove chromium. Int J Environ Sci Technol 13:327–338

Seyfu K (1997) Tef Eragrostis tef (Zucc) trotter promoting the conservation and use of underutilized and neglected crops 12 institute of plant genetics and crop plant research. Gatersleben/International Plant Genetic Resources Institute, Rome

Sharma DC, Forster CF (1994) A preliminary examination into the adsorption of hexavalent chromium using low cost adsorbents. Bioresour Technol 47:257–264

Shiow-Tien S, Norasikin S, Khairiraihanna J, Hanapi M (2014) Surface chemistry modifications of rice husk toward enhancement of Hg(II) adsorption from aqueous solution. Clean Technol Environ Policy 16:1747–1755

Simkovic I, Antal M, Alfoldi J (1994) Fractionation of wheat straw meal after pretreatment with acidified zinc chloride solutions. Carbohydr Polym 23:111–114

Srivastava VC, Mall ID, Mishra IM (2007) Adsorption thermodynamics and isosteric heat of adsorption of toxic metal ions onto bagasse fly ash (BFA) and rice husk ash (RHA). Chem Eng J 132:267–278

Suzuki M, Fujii T (1982) Concentration dependence of surface diffusion coefficient of propionic acid in activated carbon particles. AIChE J 28:380–385

Taherdanak M, Zilouei H (2014) Improving biogas production from wheat plant using alkaline pretreatment. Fuel 115:714–719

Teixeira C, Tarley R, Zezzi M, Arruda A (2004) Biosorption of heavy metals using rice milling by-products. Characterisation and application for removal of metals from aqueous effluents. Chemosphere 54:987–995

Venkatesan G, Senthilnathan U, Shameela R (2014) Cadmium removal from aqueous solutions using hybrid eucalyptus wood based activated carbon: adsorption batch studies. Clean Technol Environ Policy 16:195–200

Vermeulen T (1953) Theory for irreversible and constant pattern solid diffusion. Ind Eng Chem 45(8):1664–1670

Wassie AB, Srivastava VC (2016) Teff straw characterization and utilization for chromium removal from wastewater: kinetics, isotherm and thermodynamic modeling. J Environ Chem Eng 4:1117–1125

World Health Organization (ed) (2008) Guidelines for drinking-water quality. World Health Organization, Geneva. ISBN 9241546743

Xu J, Cheng JJ, Sharma-Shivappa RR, Burns JC (2010) Lime pretreatment of switchgrass at mild temperatures for ethanol production. Bioresour Technol 101:2900–2903

Yang H, Yan R, Chen H, Ho Lee D, Zheng C (2007) Characteristics of hemicellulose, cellulose and lignin pyrolysis. Fuel 86:1781–1788